

Composite fermion description of rotating Bose-Einstein condensates

N. R. Cooper and N. K. Wilkin

School of Physics and Astronomy, University of Birmingham, Edgbaston, Birmingham B15 2TT, United Kingdom

(Received 12 August 1999)

We study the properties of rotating Bose-Einstein condensates in parabolic traps, with coherence length large compared to the system size. In this limit, it has been shown that unusual ground states form which cannot be understood within a conventional many-vortex picture. Using comparisons with exact numerical results, we show that these ground states can be well-described by a model of noninteracting “composite fermions.” Our work emphasizes the similarities between the unusual states that appear in rotating Bose-Einstein condensates and incompressible fractional quantum Hall states. [S0163-1829(99)50148-3]

It has proved fruitful in fractional quantum Hall systems¹ to account for the many-body correlations induced by electron-electron interactions by introducing noninteracting “composite fermions.”² Recently, a similar approach has been employed to show that the correlated states arising from interparticle interactions in dilute rotating confined Bose atomic gases can be described in terms of the condensation of a type of composite *boson*.³ Here, we demonstrate that a transformation of the system of rotating bosons to that of noninteracting composite fermions is also successful in accounting for these correlated states. Our results establish a close connection between the ground states of rotating confined Bose systems and the correlated states of fractional quantum Hall systems.¹

While the trapped atom gases have been shown to Bose condense,^{4,5} the response of these condensates to rotations has not, as yet, been measured experimentally. Theoretically, it is clear that there exist various different regimes. Within the Gross-Pitaevskii framework, which requires macroscopic occupation of the single particle states, the system forms vortex arrays at both long⁶ and short⁷ coherence lengths (compared to the size of the trap), which are reminiscent of Helium-4. Here, following Ref. 3, we choose to study the system in the limit of large coherence length without demanding macroscopic occupation numbers. This allows us to study both the regime considered in Ref. 6, as well as regimes of higher vortex density where the quantum mechanical nature of the vortices will be most prevalent. Indeed, in Ref. 3 it was shown that, in general, the ground states of the rotating boson system cannot be described within a conventional many-vortex picture. Rather, the system was found to be better described in terms of the condensation of “composite bosons”—bound states of vortices and atoms—across the whole range of vortex density. In the present paper, we show that a description in terms of noninteracting composite particles with *fermionic* statistics also provides a highly accurate description of the rotating Bose system: specifically, it enables us to predict many of the features in the energy spectrum and to form good overlaps with the exact ground-state wave functions. In addition, this description indicates a close relationship between the properties of rotating Bose systems and those of fractional quantum Hall systems.

In a rotating reference frame, the standard Hamiltonian for N weakly interacting atoms in a trap is⁵

$$\mathcal{H} = \frac{1}{2} \sum_{i=1}^N \left[-\nabla_i^2 + r_i^2 + \eta \sum_{j=1, \neq i}^N \delta(\mathbf{r}_i - \mathbf{r}_j) - 2\boldsymbol{\omega} \cdot \mathbf{L}_i \right], \quad (1)$$

where we have used the trap energy, $\hbar\sqrt{K/m} = \hbar\omega_0$ as the unit of energy and the extent, $(\hbar^2/MK)^{1/4}$, of the harmonic oscillator ground state as the unit of length. (M is the mass of an atom and K the spring constant of the harmonic trap.) The coupling constant is defined as $\eta = 4\pi\bar{n}a(\hbar^2/MK)^{-1/2}$, where \bar{n} is the average atomic density and a the scattering length. The angular velocity of the trap, ω , is measured in units of the trap frequency.

Throughout this work, we make use of the limit of weak interactions ($\eta \ll 1$). It was shown in Ref. 8 that in this limit the system may be described by a two-dimensional model with a Hilbert space spanned by the states of the lowest Landau level: $\psi_m(\mathbf{r}) \propto z^m \exp(-z\bar{z}/2)$, where m is the angular momentum quantum number ($m=0,1,2,\dots$) and $z \equiv x + iy$. The kinetic energy is quenched and the ground state is determined by a balance between the interaction and potential energies. Noting that the z component of the angular momentum, L , commutes with the Hamiltonian, the total energy, scaled by η , may be written

$$E/\eta = V_N(L) + (1 - \omega)/\eta L, \quad (2)$$

where $V_N(L)$ is the interaction energy at angular momentum L . While this separation holds for all energy eigenstates, we choose $V_N(L)$ to denote the smallest eigenvalue of the interactions at angular momentum L . Since the interactions are repulsive, $V_N(L)$ decreases as L increases and the particles spread out in space; a tendency that is opposed by the term $(1 - \omega)/\eta L$ describing the parabolic confinement. Thus, as the rotation frequency ω is varied, the ground-state angular momentum will increase, from $L=0$ at $\omega=0$, to diverge as $\omega \rightarrow 1$ (when the trap confinement is lost); our goal is to describe the sequence of states (of different L) through which it passes.

We have obtained the ground-state interaction energies, $V_N(L)$, for $N=3$ to 10 particles, from exact numerical diagonalizations within the space of bosonic wave functions in the lowest Landau level.⁹ While the interaction energy $V_N(L)$ does decrease with increasing angular momentum, it is not a smooth function of L . Thus, the ground-state angular momentum, obtained by minimizing Eq. (2), is not a smoothly increasing function of ω . As shown in Fig. 1, certain values of angular momentum, corresponding to downward cusps in $V_N(L)$, are particularly stable, and are selected as the ground state over a range of ω .

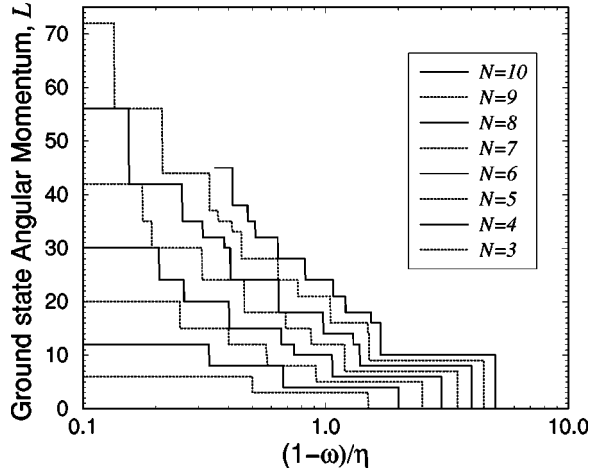


FIG. 1. Ground state angular momentum as a function of rotation frequency, ω , for $N=3 \rightarrow 10$ particles (Ref. 9).

The existence of certain angular momentum states of enhanced stability is reminiscent of the ‘‘magic values’’ of angular momentum for electrons in quantum dots,^{10–13} by analogy we will also refer to the stable angular momenta of the bosons as the magic values. Indeed, the system of bosons we study is precisely the *bosonic* variant of the (fermionic) problem of a parabolic quantum dot in strong magnetic field, with ω_0 playing the role of the magnetic field and $(1-\omega)/\eta$ the role of the parabolic confinement, and with δ -function interactions replacing the more usual Coulomb repulsion. As we shall explain, the magic values of angular momenta for the bosonic and fermionic systems are, in fact, closely related. This is a corollary of our principal result, to which we now turn, that much of the structure appearing in Fig. 1 can be interpreted simply in terms of the formation of bound states of bosons and vortices behaving as noninteracting composite particles with *fermionic* statistics—‘‘composite fermions’’ (CF).

It is known that, for *homogeneous systems*, interacting bosons and interacting fermions within the lowest Landau level have many features in common. For example, there exist certain filling fractions¹⁴ of both the boson and fermion systems at which interactions lead to incompressible ground states, with wave functions that may be related by a simple statistical transformation if $1/\nu_F = 1/\nu_B + 1$,¹⁵ (ν_B and ν_F are the filling fractions of the bosons and fermions). These similarities arise from the remarkable effectiveness of mean-field approximations to Chern-Simons theories of such systems.² Here, we are interested in an *inhomogeneous* system, in which the bosons are subject to a parabolic confinement. Jain and co-workers^{13,16,17} have shown that the fermionic equivalent of this problem—interacting electrons in a quantum dot—can be well-described in terms of properties of *noninteracting composite fermions*. Motivated by the success of their theory, we apply a similar transformation to describe the present bosonic problem.

Specifically, we make the following ansatz for the many-boson wave function:

$$\Psi_L^{\text{ansatz}}(\{z_i\}) = \mathcal{P} \left\{ \prod_{i < j} (z_i - z_j) \Psi_{L_{CF}}^{CF}(\{z_i\}) \right\}, \quad (3)$$

where $\Psi_{L_{CF}}^{CF}(\{z_i\})$ is a wave function for some fermionic particles—the composite fermions. Multiplication of the an-

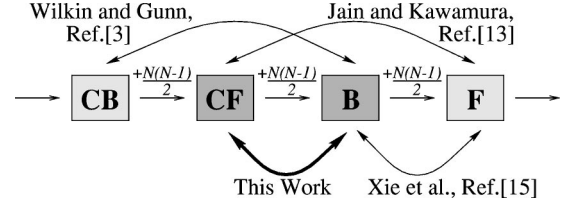


FIG. 2. A schematic relating the transformation we are performing to those that have been used previously.

tisymmetric CF wave function by the Jastrow prefactor generates a completely symmetric bosonic wave function. \mathcal{P} projects the wave function onto the lowest Landau level, which amounts to the replacement $z_i^n z_i^m \rightarrow \{(n!/m!)z_i^{n-m} (n \geq m); 0 (n < m)\}$ for all terms in the polynomial part of the wave function. For a full discussion, see Ref. 18. (For ease of presentation, we omit exponential factors and normalization constants from all wave functions.)

The transformation (3) causes the boson wave function to describe a vortex around the position of each other particle in addition to the motions described by Ψ^{CF} . One can therefore interpret a composite fermion as a bound state of a boson with a vortex of fermionic statistics (cf. Ref. 19). As a result, the angular momentum of the bosons, L , is increased with respect to that of the composite fermions, L_{CF} , according to

$$L = L_{CF} + N(N-1)/2. \quad (4)$$

Note that the transformation (3) relates $1/\nu_{CF} = 1/\nu_B - 1$ and is not the same as that used in Ref. 15. There are an unlimited number of fermion \leftrightarrow boson mappings that one can effect through transformations of the form (3). In Fig. 2 we present a schematic of how, by subsequent attachments of vortices—each causing an addition of $N(N-1)/2$ to the angular momentum—one can transform from the composite bosons (CB) introduced in Ref. 3 to the composite fermions used here (CF), to the bare boson system in which we are interested (B), and finally to a fermion system (F).

We introduce the fermion system (F) to point out that the composite fermions (CF) which we use to describe the boson system (B) are the same as those used by Jain and Kawamura¹³ to describe interacting electrons in quantum dots (F). The predictions of the energy spectrum flowing from a model of noninteracting composite fermions will therefore be identical in the boson and fermion systems up to the shift $L_F = L + N(N-1)/2$.

In the spirit of Ref. 13, we shall consider the CF’s, described by $\Psi_{L_{CF}}^{CF}(\{z_i\})$, to be noninteracting, and look at the variation of the minimum *kinetic* energy of the CF’s as a function of the total angular momentum. We further assume that a composite fermion in the Landau level state (n, m) (with Landau level index $n = 0, 1, 2, \dots$, and angular momentum $m = -n, -n+1, \dots$) has an energy $E_n = (n + 1/2)E_{CF}$, where E_{CF} is some effective cyclotron energy. These assumptions may be viewed as a mean-field treatment of the appropriate Chern-Simons theory for this system; ultimately, they are justified by the predictive successes of the resulting theory.

Figure 3 shows the resulting ground-state energy of noninteracting CF’s as a function of $L = L_{CF} + N(N-1)/2$ for $N=7, 8, 9$, together with the exact interaction energies $V_N(L)$.

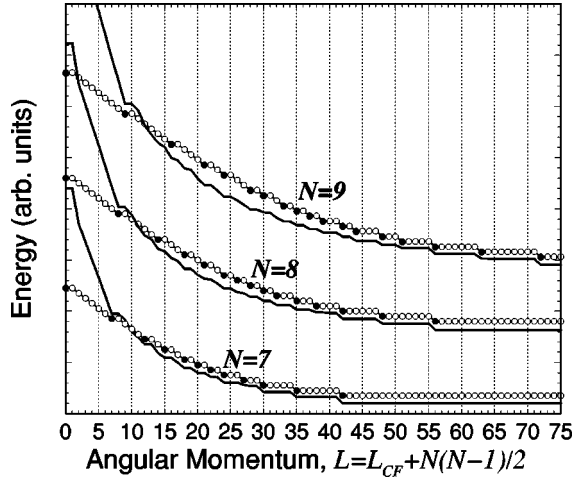


FIG. 3. The circles show the ground-state energies of noninteracting composite fermions as a function of angular momentum, for $N=7,8,9$ (filled circles identify the sets, L_N^* , of angular momenta at which the CF energy has a downward cusp). The exact interaction energies, $V_N(L)$ are shown as solid lines for comparison. (All curves are offset for clarity.)

It is apparent that the composite fermion energies fail to capture the rapid rise in the exact energies at small angular momenta; this can be interpreted as a failing of the assumption of a constant effective cyclotron energy E_{CF} . The principal success of this approach is the identification of the *cusps* in the exact energy $V_N(L)$: at almost all of the angular momenta for which the composite fermion kinetic energy shows a downward cusp (we label these sets of angular momenta by L_N^*), there is a corresponding cusp in the exact energy $V_N(L)$. Since a “magic” angular momentum of the boson system must coincide with a downward cusp in $V_N(L)$, the set L_N^* represents a set of candidate values for the magic angular momenta. For example: for $N=7$, the CF model predicts all nine actual magic numbers and in addition identifies cusps which do not become ground states for a further three $L \in L_7^*$. These missing values are not necessarily a failing of the composite fermion model. The main failing, to which we will return later, is that there is a small number of magic angular momenta that are not identified.

Not only does the composite fermion model successfully identify the majority of the magic angular momenta, as we now show it also provides a very accurate description of the associated wave functions. The composite fermion wave functions corresponding to the angular momenta L_N^* are the “compact states” discussed in Ref. 13. For these states, the composite fermions occupy the lowest available angular momentum states within each Landau level. As an illustration, for $N=4$, there is a cusp in the composite fermion energy at $L=8$ ($L_{CF}=2$), at which the composite fermions occupy the single particle states $(n,m)=\{(0,0),(0,1),(0,2),(1,-1)\}$. The wave function $\Psi_{L_{CF}}^{CF}$ is formed as a Slater determinant of these states, and the bosonic wave function Ψ_L^{ansatz} is constructed via Eq.(3).

In the cases $L=0$ and $L=N(N-1)$, this procedure yields the exact ground-state wave function for all N . At $L=0$, there is only one many-body state within the lowest Landau level (all bosons occupy the $m=0$ state); the ansatz (3) has nonzero overlap with this state, so must (trivially) be the

ground state. For $L=N(N-1)$, the lowest energy composite fermion state is formed from the states $\{(0,0),(0,1), \dots (0,N)\}$. The Slater determinant of these states may be written $\Psi^{CF}=\prod_{i<j}(z_i-z_j)$, which, inserted in Eq. (3), generates the bosonic Laughlin state $\Psi^{ansatz}=\prod_{i<j}(z_i-z_j)^2$. (This state is in the lowest Landau level, and projection is unnecessary.) Since this wave function vanishes for $z_i=z_j$ ($i \neq j$), it is the exact zero energy eigenstate of the δ -function two-body interaction potential.

At intermediate values of the angular momentum, our ansatz (3) is not, in general, exact. We have performed numerical calculations to determine the overlaps of the ansatz wave functions with the exact ground-state wave functions, $|\langle \Psi_L^{ansatz} | \Psi_L^{exact} \rangle|$. We list these overlaps in Table I at each of the angular momenta, $L \in L_N^*$, selected by the noninteracting composite fermion model. In general, the ansatz (3) has an overlap of close to unity with the exact ground state: the composite fermion model provides an excellent description of these states. Small overlaps can occur when the composite fermion model does not produce a unique ansatz, i.e., when two, or more, sets of single particle states for the composite fermions have the same kinetic energy at a given L (e.g., $N=6, L=12$). In these cases, the overlaps could be improved by diagonalizing the Hamiltonian within the space of states spanned by the two ansatz states.

Owing to the impressive agreement between the ansatz wave functions (3) and the exact ground states at L_N^* , an accurate description of the ground-state angular momentum as a function of rotation frequency can be obtained using only this set of ansatz wave functions. Minimizing the expectation value of the energy (2) within this set of ansatz wave functions, one obtains a ground-state angular momentum as a function of $(1-\omega)/\eta$ that is in excellent agreement with the exact results shown in Fig. 1. This approach does, however, omit a small number of magic angular momenta. In some cases, these are magic values identified by the composite fermion model, but for which the expectation value of the energy happens not to be sufficiently low to become stable ($N=6, L=12$; $N=9, L=33,37$; $N=10, L=38$). The most important omissions are the magic angular momenta at $N=8, L=12$, $N=10, L=16,21$ for which there are no features in the composite fermion kinetic energy that would suggest a stable angular momentum state. We believe that this emergent structure at larger numbers of particles represents many-body correlations that are not captured by the noninteracting composite fermion model used here. (Some of these states are correctly identified by the composite boson approach.³) They could be related to the incompressible states, such as $\nu=4/5$, of quantum Hall systems which cannot be explained in terms of noninteracting composite fermions alone, but require an additional “particle-hole” transformation. This view is strengthened by the observation that related magic angular momenta also appear in the exact ground-state energy of electrons in quantum dots interacting by Coulomb forces, up to the shift $L_F=L+N(N-1)/2$ (e.g., Ref. 17 identifies a stable state of $N=10$ electrons at $L_F=61$ —equivalent to $N=10, L=16$ of the present bosonic model). The study of this additional structure is beyond the scope of the present work.

TABLE I. For each number of bosons, N , the angular momenta, L_N^* , at which the noninteracting composite fermion description predicts a downward cusp are given, together with (in brackets) the overlaps of the ansatz wave function (3) with the exact ground-state wave function. Where a given angular momentum appears more than once for fixed N , the composite fermion model provides more than one candidate ground state.

| N | Angular momentum L , [$ \langle \Psi_L^{ansatz} \Psi_L^{exact} \rangle $] |
|-----|--|
| 3 | 0 [1], 3 [1], 6 [1] |
| 4 | 0 [1], 4 [0.980], 6 [0.980], 8 [0.997], 12 [1] |
| 5 | 0 [1], 5 [0.986], 8 [0.983], 10 [0.986], 12 [0.979], 15 [0.996], 20 [1] |
| 6 | 0 [1], 6 [0.989], 10 [0.956], 12 [0.770], 12 [0.745], 15 [0.977], 18 [0.981], 18 [0.240], 20 [0.978], 24 [0.996], 30 [1] |
| 7 | 0 [1], 7 [0.992], 12 [0.931], 15 [0.971], 18 [0.952], 20 [0.948], 22 [0.920], 24 [0.970], 27 [0.963], 30 [0.979], 35 [0.996], 42 [1] |
| 8 | 0 [1], 8 [0.993], 14 [0.886], 18 [0.959], 21 [0.915], 24 [0.960], 26 [0.917], 28 [0.946], 28 [0.072], 30 [0.943], 32 [0.917], 35 [0.963], 38 [0.972], 42 [0.980], 48 [0.996], 56 [1] |
| 9 | 0 [1], 9 [0.994], 16 [0.861], 21 [0.926], 24 [0.541], 24 [0.854], 28 [0.944], 30 [0.795], 30 [0.388], 33 [0.912], 35 [0.937], 37 [0.899], 39 [0.911], 42 [0.074], 42 [0.927], 44 [0.917], 48 [0.081], 48 [0.958], 51 [0.978], 56 [0.981], 63 [0.996], 72 [1] |
| 10 | 0 [1], 10 [0.995], 18 [0.848], 24 [0.853], 28 [0.934], 32 [0.907], 35 [0.902], 38 [0.872], 40 [0.733], 40 [0.607], 42 [0.016], 42 [0.577], 42 [0.779], 45 [0.894] . . . 90 [1] |

In summary, we have studied the properties of rotating Bose systems in parabolic traps in the limit of large coherence length. Through comparisons with exact results for small systems, we showed that many of the features of the exact spectrum of the bosons can be understood in terms of *noninteracting composite fermions*. The noninteracting composite fermion model leads to (i) the identification of a set of candidate values for the stable angular momenta of the bosons, and (ii) associated many-body wave functions that

have large overlap with the exact ground-state wave functions. The success of the mapping to composite fermions indicates that the ground states of rotating Bose-Einstein condensates, in the limit of large coherence length, are closely related to the correlated states appearing in fractional quantum Hall systems.

We would like to thank J.M.F. Gunn and R.A. Smith for many helpful discussions. This work was supported by the Royal Society and EPSRC GR/L28784.

¹*The Quantum Hall Effect*, edited by R. E. Prange and S. M. Girvin, 2nd ed. (Springer-Verlag, Berlin, 1990).

²*Composite Fermions: A Unified View of the Quantum Hall Effect*, edited by O. Heinonen (World Scientific, River Edge, N.J., 1998); *Perspectives in Quantum Hall Systems*, edited by S. Das Sarma and A. Pinczuk (Wiley, New York, 1997).

³N. K. Wilkin and J. M. F. Gunn, cond-mat/9906283, Phys. Rev. Lett. (to be published).

⁴M. H. Anderson *et al.*, Science **269**, 198 (1995).

⁵F. Dalfovo, S. Giorgini, L. P. Pitaevskii, and S. Stringari, Rev. Mod. Phys. **71**, 463 (1999).

⁶D. A. Butts and D. S. Rokhsar, Nature (London) **397**, 327 (1999).

⁷Y. Castin and R. Dum, Eur. Phys. J. D **7**, 399 (1999).

⁸N. K. Wilkin, J. M. F. Gunn, and R. A. Smith, Phys. Rev. Lett. **80**, 2265 (1998).

⁹These results were obtained from a combination of complete diagonalizations and Lanczos techniques. The results are limited

to $L \leq 45$ for $N = 10$.

¹⁰W. Lai, K. Yu, Z. Su, and L. Yu, Solid State Commun. **52**, 339 (1984).

¹¹P. A. Maksym and T. Chakraborty, Phys. Rev. Lett. **65**, 108 (1990); P. A. Maksym, Physica B **184**, 385 (1993).

¹²S. R. E. Yang, A. H. MacDonald, and M. D. Johnson, Phys. Rev. Lett. **71**, 3194 (1993).

¹³J. K. Jain and T. Kawamura, Europhys. Lett. **29**, 321 (1995).

¹⁴The filling fraction, ν , is defined as the ratio of the average number density of particles, to the average number density of magnetic flux quanta piercing the plane.

¹⁵X. C. Xie, S. He, and S. Das Sarma, Phys. Rev. Lett. **66**, 389 (1991).

¹⁶R. K. Kamilla and J. K. Jain, Phys. Rev. B **52**, 2798 (1995).

¹⁷T. Kawamura and J. K. Jain, J. Phys. C **8**, 2095 (1996).

¹⁸J. K. Jain, Phys. Rev. B **41**, 7653 (1990).

¹⁹N. Read, Surf. Sci. **362**, 7 (1996).